

Winter intensification of the moist branch of the circulation in simulations of 21st century climate

F. Laliberté¹ and O. Pauluis¹

Received 5 August 2010; revised 3 September 2010; accepted 17 September 2010; published 28 October 2010.

[1] In this paper, changes in isentropic circulations associated with global warming in the A1B model outputs for the 20th and 21st centuries are analyzed. The changes in the circulations on dry and moist isentropes are quantified through the use of three bulk measures of the circulations: mass transport, entropy transport and effective stratification. The circulation on dry isentropes is expected to weaken due to a reduction of the meridional heat transport and to an increase in stratification. In contrast, the moist branch of the circulation, measured in terms of the difference between the circulations on moist and dry isentropes, strengthens during the winter months. This intensification is characterized not only by an increase in the eddy latent heat transport but also by an increase in the mass transport. This indicate a larger poleward mass flow of warm moist subtropical air into the stormtracks leading to enhanced moist ascent within baroclinic eddies. **Citation:** Laliberté, F., and O. Pauluis (2010), Winter intensification of the moist branch of the circulation in simulations of 21st century climate, *Geophys. Res. Lett.*, 37, L20707, doi:10.1029/2010GL045007.

1. Introduction

[2] Climate change through this century is expected to be associated, among other things, with a change in the atmospheric energy, entropy and water vapor transports. A fundamental issue is to understand how such changes in atmospheric transports are tied with changes in the atmospheric circulation itself. For example, a larger energy transport can be associated with an increase in the overall mass transport or, alternatively, with an increase in the energy transported per unit mass of air. Several studies [e.g., Held and Soden, 2006; Mitas and Clement, 2006; Vecchi and Soden, 2007; Chou and Chen, 2010] have investigated changes in the tropical circulation due to global warming. Using twentieth century and A1B scenario twenty-first century model runs, Held and Soden [2006] observe that the increase in atmospheric water lead to a rapid increase in the tropical stratification, of approximately 7%/K, consistent with the Clausius-Clapeyron (CC) relationship. In contrast, the poleward energy transport by the circulation only increases by 2%, which thus implies a reduction of the mass transport in the Hadley cell by about 5%. With the use of a different ensemble of models, Mitas and Clement [2006] show trends for the twentieth century

indicating a statistically significant weakening of the winter Hadley cell.

[3] The arguments presented by Held and Soden [2006] are valid for the tropical regions where the mean overturning circulation dominate the energy transport. However, the same transport in the midlatitudes is dominated by large-scale eddies. In this paper, a new set of diagnostics based on the circulations on dry and moist isentropes are introduced to characterize the changes in mass and entropy transports, with the later being viewed here as an ersatz for the energy transport. As entropy can be viewed as approximately conserved over an eddy lifecycle (3–7 days), isentropic averages capture more closely the mean parcel trajectory than an Eulerian mean. We compare the circulation on dry isentropes, which can be thought of as surfaces of constant potential temperature θ , with that on moist isentropes, similar to surfaces of constant equivalent potential temperature θ_e . The two circulations differ in their relative strength, with the moist circulation being more vigorous in the midlatitudes due to the ascent of moist air within the stormtracks [Pauluis et al., 2008, 2010]. By using these new diagnostics, one can better assess how the different components of the atmospheric circulation might evolve over the next century.

2. Circulation Indices

[4] Here, we follow Pauluis et al. [2010] and process our data using the dry entropy, s_l , and the moist entropy, s_m , respectively. On a qualitative level, dry isentropes are close to surfaces of constant dry static energy and moist isentropes are close to surfaces of moist static energy, and the dry and moist entropy transports are similar to the dry and moist static energy transports. One could use the static energy instead of entropy, as in the work of Czaja and Marshall [2006], though this comes at the cost of losing the exact conservation of entropy for reversible adiabatic motions.

[5] The dry streamfunction, $\Psi_d(\phi, s_l)$, is defined as the meridional mass flux, through a latitude band, of air parcels with dry entropy values less than s_l :

$$\Psi_d(\phi, s_l) = \frac{a \cos \phi}{g} \left\langle \int_0^{p_{\text{surf}}} v H(s_l - s_l(p, \lambda, \phi, t)) dp \right\rangle, \quad (1)$$

where $\langle \cdot \rangle$ is a zonal and temporal mean; the function $H(x)$ is the Heaviside function, which is 1 when $x \geq 0$ and 0, otherwise; a denotes the earth's radius, g the gravitational acceleration; and p , λ , ϕ are the pressure, zonal and meridional coordinates, respectively. The surface pressure p_{surf} and the meridional velocity v are obtained from gridded data.

[6] The moist streamfunction, $\Psi_m(\phi, s_m)$, can be similarly defined using the moist entropy. In order to synthesize some

¹Courant Institute of Mathematical Sciences, New York University, New York, New York, USA.

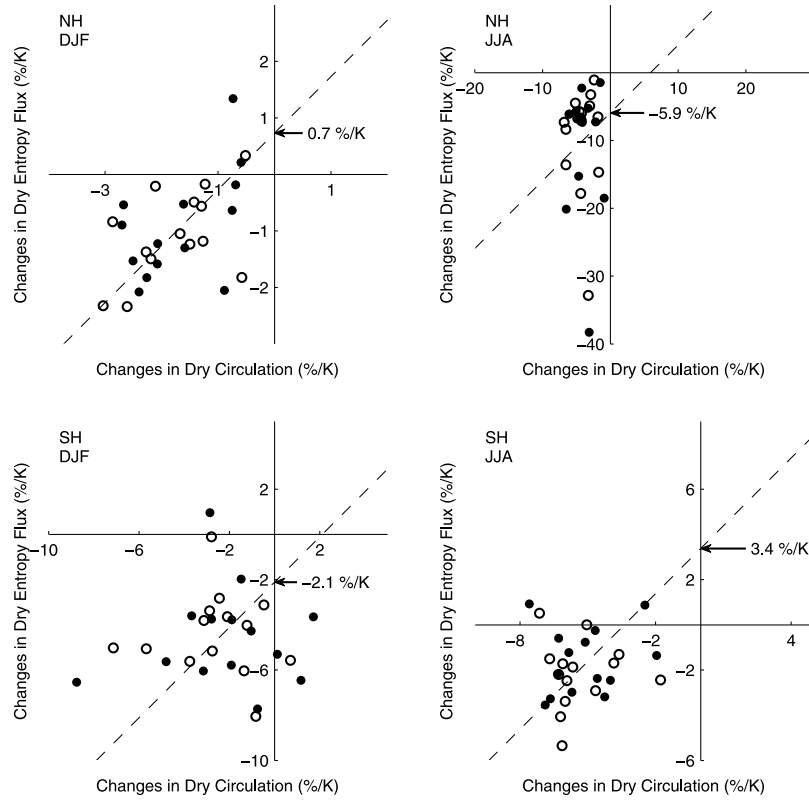


Figure 1. Relative changes in the dry transport. On the ordinate are plotted changes in fluxes while on the abscissa are plotted changes in circulations. On each graph, the arrow indicates the mean relative changes in stratification as defined by (6), which can be read off the intersection of the dashed line of slope unity with the ordinate. Filled dots correspond to changes between 1961–2000 and 2046–2065 while empty dots correspond to changes between 1961–2000 and 2081–2100. See Table 2 for ensemble averages and standard deviations.

features of the circulation, we extract a small number of indices from the full streamfunctions Ψ_d and Ψ_m . The total mass transport on s_l , $\Delta\Psi_d$, is defined by:

$$\Delta\Psi_d(\phi) = \max_{s_l} \{\Psi_d(\phi, s_l)\} - \min_{s_l} \{\Psi_d(\phi, s_l)\}. \quad (2)$$

The dry entropy transport is given by:

$$F_{s_l}(\phi) = \frac{a \cos \phi}{g} \left\langle \int_0^{p_{\text{surf}}} s_l v dp \right\rangle. \quad (3)$$

A similar expression can be found for $\Delta\Psi_m$ and F_{s_m} by replacing s_l with s_m in (2) and (3).

[7] We have chosen to rely on bulk quantities averaged over the regions 25°N–60°N and 60°S–25°S. As presented by Pauluis *et al.* [2010], in these regions $\Delta\Psi_m$ dominates $\Delta\Psi_d$. We define the *total circulation index* as the average value

$$\overline{\Delta\Psi_m}^N = \frac{1}{35} \int_{25^\circ\text{N}}^{60^\circ\text{N}} \Delta\Psi_m(\phi) d\phi. \quad (4)$$

Note that the differential area element is implicitly included in (1), making this average area-weighted.

[8] For our analysis, we also require a measure of the entropy transport, F_{s_m} , over these regions. Using the same average as for (4), we define

$$\overline{F_{s_m}}^N = \frac{1}{35} \int_{25^\circ\text{N}}^{60^\circ\text{N}} F_{s_m}(\phi) d\phi, \quad (5)$$

which, in turn, enables us to find a related hemisphere-wide *effective stratification* [Pauluis *et al.*, 2010], Δs_m :

$$\Delta s_m^N = \frac{\overline{F_{s_m}}^N}{\overline{\Delta\Psi_m}^N}. \quad (6)$$

The effective stratification (6) measures the difference of s_m between the poleward branch and the equatorward branch of the circulation. It depends not only on vertical stratification, but also on horizontal fluctuations of s_m in the midlatitude eddies. Quantities (4), (5) and (6) can be extended for the *dry circulation and the southern hemisphere*. We will refer to $\overline{\Delta\Psi_d}^N$ and $\overline{\Delta\Psi_d}^S$ as the *dry branch indices*.

[9] Pauluis *et al.* [2010] show that the difference between the transport on s_m and on s_l is associated with a poleward mass flow of warm subtropical air that ascends through the stormtracks. The enhanced mass transport on s_m , $\Delta\Psi_m(\phi) - \Delta\Psi_d(\phi)$, is used here to quantify the ascent of moist air within the stormtracks. The difference $F_{s_m}(\phi) - F_{s_l}(\phi)$ is

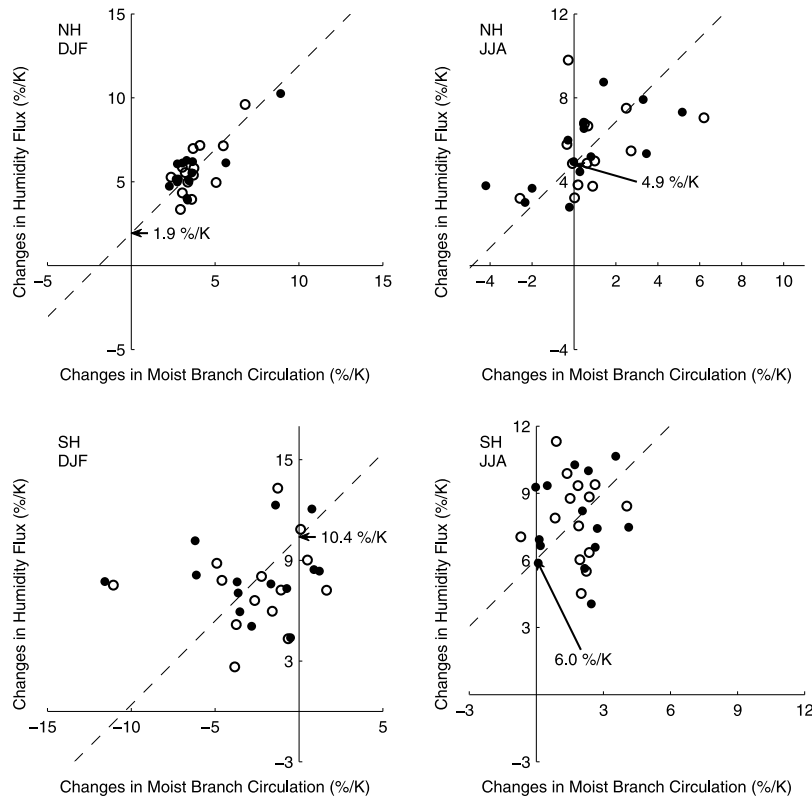


Figure 2. Relative changes in the moist branch transport. Same as in Figure 1 but for the moist branch transport. The stratification is defined by (7).

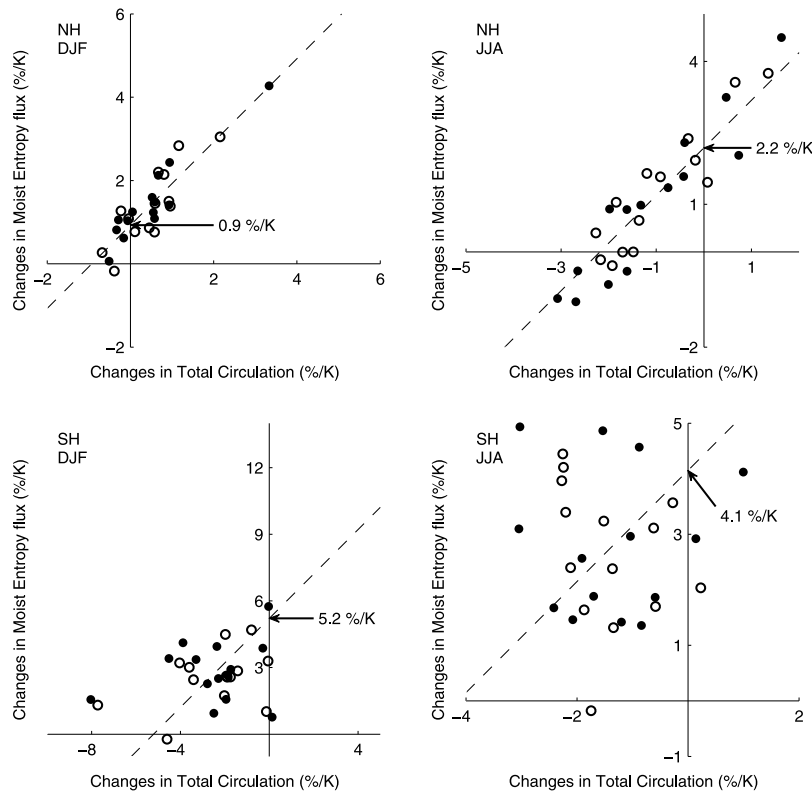


Figure 3. Relative changes in the total transport. Same as in Figure 1 but for the total transport.

Table 1. List of Analyzed Models With Daily Output^a

Laboratory	Model
GFDL, USA	cm 2.0
GFDL, USA	cm 2.1
CNRM, France	cm 3
CSIRO, Australia	mk 3.5
GISS, USA	Model ER
MIROC, Japan	3.2 Medres
MIROC, Japan	3.2 Hires
MIUB, Germany	echo G
MPI, Germany	echam 5
MRI, Japan	cgcm 3.2.2a
CCCMA, Canada	cgcm 3.1 t63
IPSL, France	cm 4
INGV, Italy	echam 4
NCAR, USA	ccsm 3.0

^aModels are listed by their laboratory of origin and their model numbers.

proportional to the difference of q_T between the poleward flow and the equatorward flow, multiplied by the mass transport within the moist branch. Finally, an effective moisture stratification is defined as

$$\overline{\Delta q_T}^N = \frac{\overline{F_{s_m}^N} - \overline{F_{s_l}^N}}{\overline{\Delta \Psi_m}^N - \overline{\Delta \Psi_d}^N}, \quad (7)$$

an expression that is proportional to the difference in specific humidity between the poleward and equatorward flows.

3. Data

[10] We use results from the World Climate Research Programme's (WCRP's) Coupled Model Intercomparison Project phase 3 (CMIP3) multi-model data set, based on the Intergovernmental Panel on Climate Change (IPCC) Fourth Assessment Report (AR4) A1B scenario. Seasonal averages of (4) and (5) were computed for the twentieth century 1961–2000 and A1B scenario twenty-first century 2046–2065 and 2081–2100 periods. Changes between 2046–2065 and 1961–2000 as well as between 2081–2100 and 1961–2000 were computed for each models in Table 1. In Figures 1, 2, and 3, we present our results as scatter plots for both hemispheres and both solstice seasons, JJA and DJF. Color versions of Figures 1, 2, and 3 allowing the identification of individual models are provided as Figures S1–S3 of the auxiliary material, respectively, with their accompanying legend as Figure S4.¹ For each analyzed model, two data points will appear in each plot, one — filled — for the change between 1961–2000 and 2046–2065, and a second — not filled — for the change between 1961–2000 and 2081–2100, and the numerical values for the mean and variance of the model ensemble are presented in Table 2.

4. Results

[11] Figure 1 shows the changes in dry entropy transport versus changes in the dry circulation for DJF and JJA of both hemispheres. In all cases, most models are found in the third quadrant, corresponding to a reduction in dry entropy transport and a reduction in mass transport by the dry branch. The mass transport weakens with changes between

–1.7%/K and –5.3%/K. The weakening is less pronounced in the Winter hemispheres. There is also a large inter-model spread in the prediction for the northern summer, which is explained in part by the fact that the circulation on s_l is at its weakest during this season, and is thus most sensitive to large fluctuations. The dry entropy transport only weakens significantly during the summer season (–9.9%/K in the North and –4.5%/K in the South), and much less (–1.0%/K and –1.9%/K, respectively) during the winter.

[12] The change in effective stratification can be obtained by subtracting the change in mass transport from the change in dry entropy transport:

$$\frac{1}{\overline{\Delta s_l}^N} \frac{\delta \overline{\Delta s_l}^N}{\delta T} = \frac{1}{\overline{F_{s_l}^N}} \frac{\delta \overline{F_{s_l}^N}}{\delta T} - \frac{1}{\overline{\Delta \Psi_d}^N} \frac{\delta \overline{\Delta \Psi_d}^N}{\delta T}. \quad (8)$$

In equation (8), $\delta(\cdot)$ refers to the value in one of the period of the twenty-first century minus the corresponding value in the twentieth century. The temperature T corresponds to the area-weighted average surface temperature over the same regions (60°S–25°S and 25°N–60°N).

[13] In Figure 1, the dashed line with slope unity indicates the mean value for the change in stratification, which can be read at its intersection with the ordinate axis. The stratification increases in the Southern hemisphere by 3.4%/K in the summer, and decreases by –2.1%/K during the winter. Changes in the stratification are less pronounced during Northern winter (increasing by 0.7%/K) and unreliable during the Northern summer, where the dry circulation is particularly weak. In all cases, these changes are significantly less than the expected changes in tropical stratification associated with CC scaling. In contrast to the changes in the tropical circulation noted by *Held and Soden* [2006], the weakening of mass transport on dry isentropes in the mid-latitudes appears to primarily due to a reduction of the poleward transport of dry entropy, with a lesser impact from changes in stratification.

[14] Figure 2 shows changes in the moisture transport $\overline{F_{s_m}^N} - \overline{F_{s_l}^N}$, versus changes in the moist branch index $\overline{\Delta \Psi_m}^N - \overline{\Delta \Psi_d}^N$. The multi-model ensemble mean shows a marked increase in moisture transport in the North at 5.7%/K in DJF and 5.5%/K in JJA, and in the South at 7.7%/K in DJF and 7.8%/K in JJA. The mass transport by the moist branch

Table 2. Summary of statistics from Figures 1, 2, and 3^a

Quantity	DJF		JJA	
	North	South	North	South
Dry				
Circulation	–1.7 ± 0.8	–2.4 ± 2.3	–4.1 ± 1.7	–5.3 ± 1.5
Dry Stratification	0.7 ± 0.8	–2.1 ± 3.1	–5.9 ± 8.9	3.4 ± 2.0
Dry Entropy Fluxes	–1.0 ± 0.9	–4.5 ± 2.0	–9.9 ± 8.6	–1.9 ± 1.5
Moist Branch				
Circulation	3.8 ± 1.4	–2.7 ± 3.2	0.7 ± 2.2	1.8 ± 1.2
Moisture Stratification	1.9 ± 1.0	10.4 ± 3.8	4.9 ± 2.0	6.0 ± 2.2
Humidity Fluxes	5.7 ± 1.5	7.7 ± 2.4	5.5 ± 1.8	7.8 ± 1.9
Total				
Circulation	0.5 ± 0.8	–2.5 ± 2.0	–1.0 ± 1.2	–1.4 ± 1.0
Moist Stratification	0.9 ± 0.4	5.2 ± 2.1	2.2 ± 0.6	4.1 ± 1.7
Moist Entropy Fluxes	1.4 ± 0.9	2.7 ± 1.3	1.2 ± 1.5	2.7 ± 1.3

^aThe numbers listed indicate the ensemble average of the quantity in the first column. The error is the standard deviation from the model ensemble. We have indicated in bold the results that fall outside one standard deviation of no changes.

¹Auxiliary materials are available in the HTML. doi:10.1029/2010GL045007.

increases also significantly during the winter, by 3.8%/K in the North and 1.8%/K in the South, but decreases in the Southern summer by $-2.7\%/K$ while remaining almost unchanged (increasing by $0.7\%/K$ with a standard deviation of $2.2\%/K$) during the Northern summer. The dashed line shows the mean change in effective moisture stratification. In both hemispheres, summer eddies have a higher moisture stratification change than the winter eddies' ($4.9\%/K$ vs $1.9\%/K$ for the north and $10.4\%/K$ vs $6.0\%/K$ for the south).

[15] During summer, the increase in water vapor transport can be associated with an increase in humidity content between the dry equatorward and moist poleward flow that is roughly consistent with the CC scaling, associated with a small weakening of the mass transport. In contrast, relative changes in moisture content are smaller during winter, and the increase in water vapor transport is tied to an increase in the mass flow of warm moist air into the stormtracks. This increase in the mass transport by the moist branch of the circulation during the winter is remarkable, given that the dry circulation on s_l is expected to weaken in both the tropics and the midlatitudes. Based on these diagnostics, it is expected that through the next century, midlatitudes eddies will extract a larger amount of warm, moist subtropical air that will rise within the stormtracks. This analysis points not only to an increase in the winter precipitation in the midlatitudes, but also to an increase in the amount of air that ascends within winter storms.

[16] In Figure 3, we plot changes in the moist entropy fluxes $F_{s_m}^-$ versus changes in $\Delta\Psi_m$, the total mass transport on s_m . The change in total mass transport decreases for the Northern summer (by $-1.0\%/K$) and for the Southern hemisphere (by $-2.5\%/K$ for DJF and $-1.4\%/K$ for JJA), but increases slightly during the northern winter (by $0.5\%/K$, with a standard deviation of $0.8\%/K$). The effective stratification increases in both hemispheres and both seasons with ensemble means ranging from $0.9\%/K$ to $5.2\%/K$. The changes in total circulation are thus the result of the weakening of the dry circulation and the intensification, at least during the winter season, of the moist branch. The total circulation only increases during the Northern winter where the intensification of the moist branch more than compensates for the weakening of its dry branch.

5. Conclusion

[17] We have analyzed a subset of model outputs for the IPCC AR4 to identify changes in the midlatitude circulation. A set of indices has been introduced to characterize the mass and entropy transport by the dry and moist branch of the circulation separately, and to estimate how these would be affected by climate change over the next century. These diagnostics offer the advantage that they incorporate in a physically consistent manner the eddy transport into the overall circulation. This complements other studies such as *Teng et al.* [2008] and *Bengtsson et al.* [2009] focused on changes in individual storms, by offering an integrated assessment of the changes over many storms.

[18] In accordance with previous studies, we found that the mass transport by the dry branch weakens as temperatures increase. This behavior is qualitatively similar, although not as pronounced as the changes in the tropical Hadley circulation discussed by *Held and Soden* [2006]. We also found that the mass transport by the moist branch cir-

ulation, identified as the difference between the circulation on moist and dry isentropes, intensifies during the winter months but not during the summer months. Physically, this can be interpreted as an increase in the mass of air ascending within midlatitude winter storms.

[19] Our analysis also indicates that a weakening of the dry branch of the circulation can be in part balanced by the strengthening of the moist branch. As the dry circulation becomes inhibited by an enhanced dry stratification and weaker Equator-to-Pole temperature gradients, the moist branch can become more active, thus extracting more moist air from the subtropical regions. This suggests that in a warmer planet, even as the atmosphere becomes more stable for dry baroclinic instability, moist processes play a more significant role in the maintenance of the stormtracks. Understanding the exact nature of this compensation between the dry and moist branches remains an open question that is central to our ability to predict the evolution of the midlatitudes climate over the next century.

Appendix A: Methodology

[20] The dry and moist version of the quantities (1) and (3) were computed using the mass flux joint distribution M of *Pauluis et al.* [2008] on a 130×130 rectilinear grid $c_{pd} \ln \frac{250K}{T_0} \leq (s_l, s_m) \leq c_{pd} \ln \frac{380K}{T_0}$. The data was acquired from the CMIP3 archive of daily outputs for the 20th century and the A1B scenario [*Meehl et al.*, 2007]. The NCAR CCSM3 daily model output is an exception: it was obtained from the NCAR data repository (runs 030e and 040e). Some models were removed from our analysis, in all cases for technical reasons, including missing data.

[21] We enforced a strict mass conservation at each latitude, equivalent to demanding that the joint distribution sums to zero. At a given latitude, the exact procedure depends on whether M sums to a positive or to a negative number. If it is negative (positive, resp.), then we multiply the positive (negative, resp.) part of M by the appropriate factor to make the joint distribution sum to zero. This process can be described with the following filter:

$$M(s_l, s_m) = \max\{A, 1\} \max\{M(s_l, s_m), 0\} + \max\{A^{-1}, 1\} \min\{M(s_l, s_m), 0\}, \quad (A1)$$

$$A = \left(\int_{-\infty}^{\infty} \int_{-\infty}^{\infty} -\min\{M(s_m, s_m), 0\} ds_l ds_m \right) / \dots \left(\int_{-\infty}^{\infty} \int_{-\infty}^{\infty} -\max\{M(s_m, s_m), 0\} ds_l ds_m \right). \quad (A2)$$

[22] **Acknowledgments.** We acknowledge the modeling groups, the Program for Climate Model Diagnosis and Intercomparison (PCMDI), and the WCRP's Working Group on Coupled Modelling (WGCM) for their roles in making available the WCRP CMIP3 multi-model data set. Support of this data set is provided by the Office of Science, U.S. Department of Energy. This work was supported by the NSF grant ATM-054507. F. Laliberté was supported by a NSERC/CRSNG doctoral fellowship.

References

Bengtsson, L., K. Hodges, and N. Keenlyside (2009), Will extratropical storms intensify in a warmer climate?, *J. Clim.*, 22, 2276–2301, doi:10.1175/2008JCLI2678.1.

- Chou, C., and C-A. Chen (2010), Depth of convection and the weakening of tropical circulation in global warming, *J. Clim.*, *23*, 3019–3030, doi:10.1175/2010JCLI3383.1.
- Czaja, A., and J. Marshall (2006), The partitioning of poleward heat transport between the atmosphere and ocean, *J. Atmos. Sci.*, *63*, 1498–1511, doi:10.1175/JAS3695.1.
- Held, I. M., and B. Soden (2006), Robust responses of the hydrological cycle to global warming, *J. Clim.*, *19*, 5686–5699, doi:10.1175/JCLI3990.1.
- Meehl, G. A., C. Covey, K. E. Taylor, T. Delworth, R. J. Stouffer, M. Latif, B. McAvaney, and J. F. B. Mitchell (2007), The WCRP CMIP3 multi-model data set: A new era in climate change research, *Bull. Am. Meteorol. Soc.*, *88*, 1383–1394, doi:10.1007/s00382-007-0314-1.
- Mitas, C. M., and A. Clement (2006), Recent behavior of the hadley cell and tropical thermodynamics in climate models and reanalyses, *Geophys. Res. Lett.*, *33*, L01810, doi:10.1029/2005GL024406.
- Pauluis, O., A. Czaja, and R. Korty (2008), The global atmospheric circulation on moist isentropes, *Science*, *321*(5892), 1075–1078, doi:10.1126/science.1159649.
- Pauluis, O., A. Czaja, and R. Korty (2010), The global atmospheric circulation in moist isentropic coordinates, *J. Clim.*, *23*, 3077–3093, doi:10.1175/2009JCLI2789.1.
- Teng, H., W. Washington, and G. Meehl (2008), Interannual variations and future change of wintertime extratropical cyclone activity over North America in CCSM3, *Clim. Dyn.*, *30*, 673–686, doi:10.1007/s00382-007-0314-1.
- Vecchi, G., and B. Soden (2007), Global warming and the weakening of the tropical circulation, *J. Clim.*, *20*, 4316–4340, doi:10.1175/JCLI4258.1.

F. Laliberté and O. Pauluis, Courant Institute of Mathematical Sciences, New York University, 251 Mercer St., New York, NY 10012, USA. (lalibert@cims.nyu.edu; pauluis@cims.nyu.edu)